Rare Decays and other Electroweak b-physics Measurements at ATLAS and CMS

P. Ronchese
Università di Padova, Dipartimento di Fisica e Astronomia & INFN, Sezione di Padova
via Marzolo, 8, Padova, Italy
ATLAS and CMS Collaborations

In b quark decay the tree-level process with W exchange is hardly modified by new physics beyond the standard model; the search for new physics hints can be done exploiting the sensitivity of some processes to loop diagrams. Such processes include rare FCNC decays, whose branching ratio or angular distributions could be modified by the presence of new degrees of freedom in the loops. Another process where new physics could show itself is B_s^0 meson mixing, where the CP violation phase is predicted by SM to be very small and the observation of a significant violation would indicate the presence of new processes.

1 Introduction

Among the motivations to study heavy flavour physics at LHC experiments, and specifically CMS and ATLAS, there's the look for indirect evidence, or constraints, of new physics beyond the standard model. In b quark decay the exchange of a W boson at tree level is hardly affected by new physics processes, so the sensitivity to such processes is exploited in loop diagrams. More specifically the branching ratio of decays implying flavour-changing neutral currents can be modified by the presence of new particles circulating in the loops, while angular analysis can probe specific terms in effective lagrangian. While in decays one observes processes with flavour changes of one unit, in B^0 mixing processes with changes of two flavour units are investigated, and new physics contributions to CP violation may appear.

Both ATLAS and CMS experiments collected an integrated luminosity of about 5 fb^{-1} in 2011 at $\sqrt{s} = 7$ TeV and about 20 fb^{-1} in 2012 at $\sqrt{s} = 8$ TeV. All measurements involve dimuons; dedicated triggers requiring the presence of two muons have been developed for the analyses, to achieve a sustainable trigger rate when collecting data at the very high luminosities provided by LHC. Common selections criteria among the analyses include cuts on the dimuon mass, the requirement that the two muons form a displaced vertex and cuts on the pointing angle, that's the angle formed by the dimuon momentum and the flight direction, given by the position of the secondary vertex relative to the primary vertex.

2 Rare decays

2.1 $B_{d,s}^0 \to \mu^+\mu^-$ *branching ratio*

The decay $B_{d,s}^0 \to \mu^+\mu^-$ is a highly suppressed process in the standard model, because not only it involves a flavour-changing neutral current, but it's also Cabibbo suppressed, it's helicity suppressed and it requires an internal annihilation.

A branching ratio prediction from the standard model including new NLO electroweak corrections and NNLO QCD corrections has been recently published [1]:

$$\mathcal{B}(B_s^0 \to \mu^+\mu^-)_{\rm SM} = (3.65 \pm 0.23) \times 10^{-9}$$
$$\mathcal{B}(B_d^0 \to \mu^+\mu^-)_{\rm SM} = (1.06 \pm 0.09) \times 10^{-10}$$

Significant deviations are predicted by theories beyond the standard model, implying the presence of new degrees of freedom in the loops, as shown in fig.1, both for box and penguin diagrams.

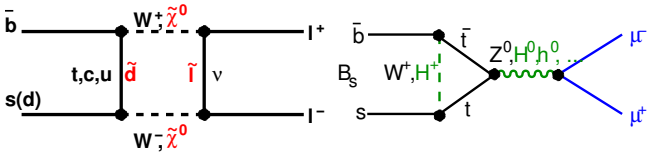

Figure 1 – $B^0_{d,s}$ decay diagrams predicted by SM and new physics models

Enhancements of the branching ratio are predicted by models with non-universal Higgs masses [2], leptoquarks [3] or MSSM with large $\tan\beta$ that can predict branching ratios proportional to $\tan\beta$ up to the $6^{\rm th}$ power [4,5]. On the contrary, other models as supersymmetry with maximum CP violation and minimum flavour violation would predict a suppression [6]. A discrimination among different theories can come from the ratio R of the two branching fractions; for example theories beyond the standard model assuming minimal flavour violation predict a value for R equal as in the standard model itself [7], so a deviation would invalidate them.

Both ATLAS and CMS measured the branching ratio by a comparison with the decay $B^\pm \to J/\psi K^\pm \to \mu^+\mu^- K^\pm$, used for normalization. In this way the uncertainties related to production cross-section and luminosity cancel out. The branching ratio of the $B^0_{d,s}$ was then obtained by the following expression:

$$\mathcal{B}(B^0_{d,s} \to \mu^+\mu^-) = \frac{N_{\rm sig}}{N_{\rm nrm}} \frac{\epsilon_{\rm nrm}}{\epsilon_{\rm sig}} \frac{f_u}{f_{d,s}} \mathcal{B}(B^\pm \to J/\psi K^\pm \to \mu^+\mu^- K^\pm)$$

where $N_{\rm sig}$ and $N_{\rm nrm}$ are the number of events in the signal and normalization samples respectively, $\epsilon_{\rm sig}$ and $\epsilon_{\rm nrm}$ are the selection efficiencies and f_u, $f_{d,s}$ are the B^+ and $B^0_{d,s}$ fragmentation functions; $f_u/f_d = 1$ was assumed while f_s/f_d was taken from LHCb measurements [8,9].

Multivariate analysis was used in the event selection both by ATLAS and CMS.

The most critical point in the measurement of the branching ratio of a decay being so rare is the background evaluation.

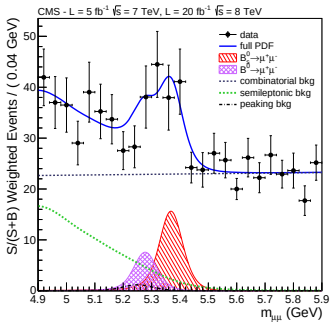

Figure 2 – Combined mass distribution for all BDT categories (CMS). This distribution is for illustrative purposes only and was not used in obtaining the final results.

Combinatorial background, represented by the grey dashed line in fig.2, was estimated using the sidebands. Physical backgrounds have been estimated using the simulations and can be

divided into non-peaking background, shown as a green line in fig.2, composed mainly from semileptonic decays of b hadrons with the final hadron misidentified as a muon, and peaking background, composed by decays of a B hadron to two light hadrons both misidentified as muons.

Fitting the distributions ATLAS set an upper limit [10]:

$$\mathcal{B}(B_s^0 \to \mu^+\mu^-) < 1.5 \times 10^{-8} @\ 95\%\ \text{C.L.}$$

while CMS measured a non zero value [11]:

$$\mathcal{B}(B_s^0 \to \mu^+\mu^-)_{\text{SM}} = (2.8^{+1.0}_{-0.9}) \times 10^{-9}$$
$$\mathcal{B}(B_d^0 \to \mu^+\mu^-)_{\text{SM}} = (4.4^{+2.2}_{-1.9}) \times 10^{-10}$$

This result changed since previously published one [12], to allow a consistent combination with the corresponding one from LHCb. The most important changed quantity is the ratio of the fragmentation functions, taken from latest LHCb measurement [9]. The estimation of the background coming from $\Lambda_b^0 \to p\mu^-\nu$ was also improved; having no measurement for the branching ratio $\mathcal{B}(\Lambda_b^0 \to p\mu^-\nu)$ the latest prediction [13] was used. The new input values, together with previously used ones, are reported in table 1.

Table 1: New input quantities used in $\mathcal{B}(B^0_{d,s} \to \mu^+\mu^-)$ measurement by CMS. An event by event weighting was applied to $\Lambda_b^0 \to p\mu^-\nu$ simulated events to account for the differences between the simulated and predicted properties of the decay.

Updated quantity	old	new
f_u/f_s	3.91 ± 0.31	3.86 ± 0.22
$\mathcal{B}(\Lambda_b^0 \to p\mu^-\nu)$	$(6.50 \pm 6.50) \times 10^{-4}$	$(4.94 \pm 2.19) \times 10^{-4}$ event by event weights

Another effect considered in the latest CMS analysis is the selection efficiency dependence on the decay time, that's not described by a simple exponential due to the fact that the B_s^0 is a superposition of two different states with different lifetimes, so a time-dependent correction was applied.

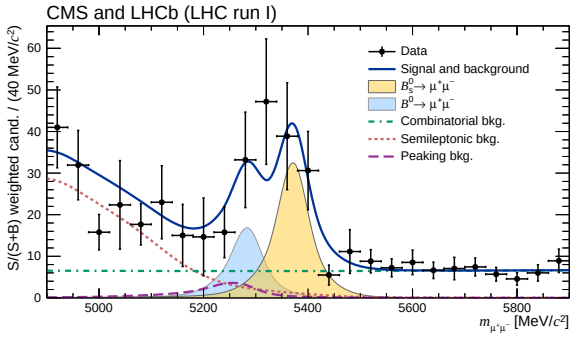

Figure 3 – Mass distribution for combined CMS and LHCb events.

In fig.3 the mass distribution of the combined events of CMS and LHCb is shown; perfoming an unique fit to the global PDF the following results have been obtained:

$$\mathcal{B}(B_s^0 \to \mu^+\mu^-)_{\text{SM}} = (2.8^{+0.7}_{-0.6}) \times 10^{-9}$$
$$\mathcal{B}(B_d^0 \to \mu^+\mu^-)_{\text{SM}} = (3.9^{+1.6}_{-1.4}) \times 10^{-10}$$

In fig.4 the comparison of the results with the standard model expectations is shown.

In the new runs LHC will operate at higher energy, up to $\sqrt{s} = 14$ TeV, that will mean higher cross-sections, and higher luminosity, up to $L = 5 \times 10^{34}$ cm^{-2}s^{-1}, that will mean larger data

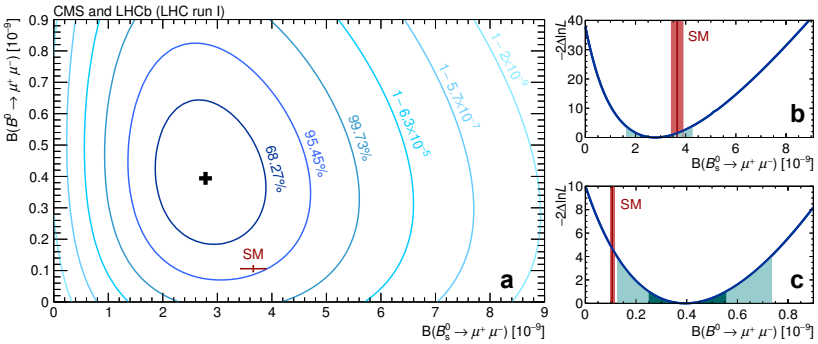

Figure 4 – Likelihood contours in the $\mathcal{B}(B_d^0 \to \mu^+\mu^-)$ versus $\mathcal{B}(B_s^0 \to \mu^+\mu^-)$ plane (a) and variations of the test statistic $-2\Delta \ln L$ for $\mathcal{B}(B_s^0 \to \mu^+\mu^-)$ and $\mathcal{B}(B_d^0 \to \mu^+\mu^-)$ (b,c respectively).

samples but also higher pileup, up to 140 interactions per bunch crossing. CMS will be upgraded to cope with the changing situation: the tracker will be improved after LS2 and for HL-LHC, and the trigger will be improved too. Despite the improvements in the tracking resolution, with high pileup a loss in efficiency can be foreseen due to the higher probability to have an additional primary vertex near the decay point; on the other side the determination of f_s/f_d is expected to improve as well as the background determination. The expected uncertainties [14] in the branching ratios measurements are reported in table 2.

Table 2: Expected uncertainties obtained by CMS in the measurement of the branching fractions $\mathcal{B}(B_s^0 \to \mu^+\mu^-)$, $\mathcal{B}(B_d^0 \to \mu^+\mu^-)$ and their ratio R.

$\mathcal{L}(\text{fb}^{-1})$	$\delta\mathcal{B}/\mathcal{B}(B_s^0 \to \mu^+\mu^-)$	$\delta\mathcal{B}/\mathcal{B}(B_d^0 \to \mu^+\mu^-)$	$\delta\mathcal{R}$
300	13%	48%	50%
3000	11%	18%	21%

2.2 $B^0 \to K^{*0}\mu^+\mu^-$ angular analysis

An angular analysis of the $B^0 \to K^{*0}\mu^+\mu^-$ decay can give hints of effects of physics beyond the standard model [15] through contributions to Wilson coefficients C_7 , C_9 and C_{10}. The differential branching ratio can be expressed as a function of 4 kinematic variables, the 3 angles θ_L , θ_K and ϕ, as shown in fig.5, and the q^2, equal to the squared dimuon mass.

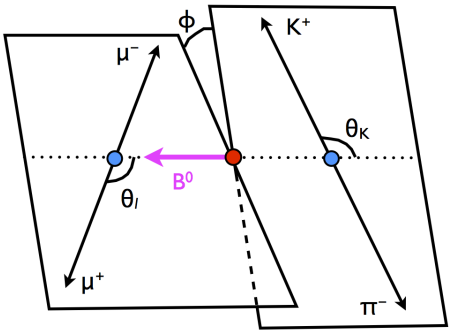

Figure 5 – Decay angles in $B^0 \to K^{*0}\mu^+\mu^-$.

In the analysis performed by ATLAS and CMS the differential decay rate is expressed using the following set of parameters: the forward-backward asymmetry (A_{FB}), the longitudinal polarization of the K^{*0} (F_{L}) and the residual S-wave contribution and interference of the $K^+\pi^-$ system (F_{S} and A_{S}). In the analysis events have been divided in q^2 square bins, the regions

corresponding to the decays $B^0 \to K^{*0}(J/\psi\ ,\psi')$ have been removed and the ϕ angle has been integrated out. Both experiments up to now gave public results only for 2011 data.

ATLAS performed a sequential fit [16]: in the first step signal yields were determined from mass fit, as shown in the fig.6, then asymmetry and polarization were obtained from angles fit, while taking S-wave contributions from BaBar measurements [17].

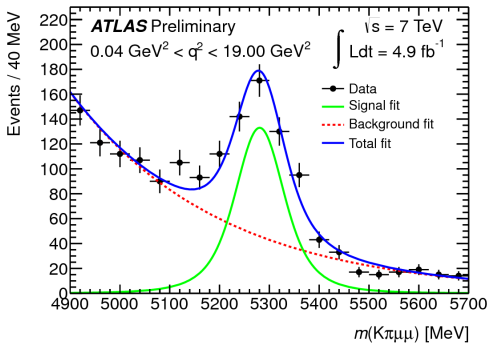

Figure 6 – Invariant mass distribution of $B^0 \to K^{*0}\mu^+\mu^-$ candidates (ATLAS). The solid blue (dark) line denotes the mass likelihood fit with the background component as dotted red line and the signal component as solid green (light) line.

CMS performed a simultaneous fit [18] to the four parameters, constraining the S-wave component to the value obtained fitting the $B^0 \to K^{*0}(J/\psi\ ,\psi')$ regions, and obtained the differential cross section dB/dq^2 by a comparison with the decay $B^0 \to K^{*0}J/\psi$:

$$\frac{d\mathcal{B}(B^0 \to K^{*0}\mu^+\mu^-)}{dq^2} = \frac{\epsilon_N}{\epsilon_S}\frac{\mathcal{B}(B^0 \to K^{*0}J/\psi)}{Y_N}\frac{dY_S}{dq^2}$$

The result of the measurement of dB/dq^2 is shown in fig.7.

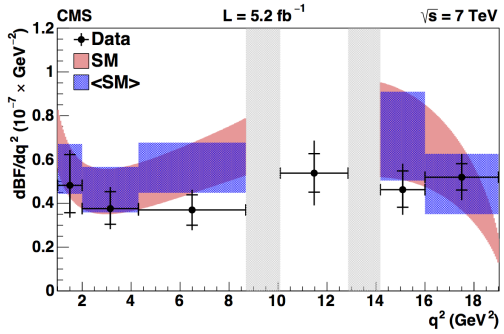

Figure 7 – Results of the measurement of dB/dq^2 versus q^2 (CMS). The statistical uncertainty is shown by inner error bars, while the outer error bars give the total uncertainty.

In fig.8 the results are shown, together with the corresponding ones obtained by previous experiments and the expectations from the standard model both for high and low q^2, while no reliable prediction is available in the mid-q^2 region. Measurements appear to be compatible both among experiments and with the expectations.

3 CP violation

3.1 $B_s^0 \to J/\psi\phi$ lifetime difference and CPV phase

In the $B_s^0 \to J/\psi\phi$ decay the flavoured initial state is an admixture of two mass eigenstates B_L^0 and B_H^0, while the final state is unflavoured, so an interference arises between the direct and mixing-mediated decays. The final state, also, does not have a definite CP, being an

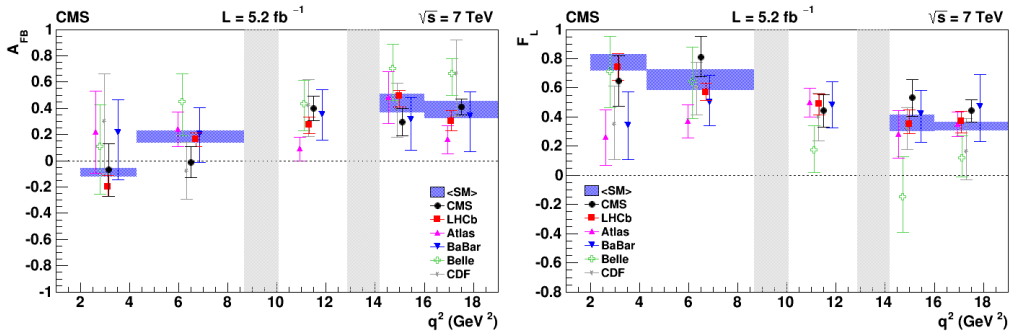

Figure 8 – Comparison of the measurement of $A_{\rm FB}$ (left) and $F_{\rm L}$ (right) versus q^2.

admixture of odd and even CP eigenstates, that must be disentangled performing again an angular analysis. The interference phase in the standard model is predicted to be $\phi_s \simeq -2\beta_s$, where $\beta_s = \arg(-(V_{ts}V_{tb}^*)/(V_{cs}V_{cb}^*)$. The latest prediction [19] for β_s is

$$2\beta_{s(\rm SM)} = 0.0363^{+0.0016}_{-0.0015}\ \text{rad}.$$

Very small deviations from the standard model expectation are also predicted by new physics models with minimal flavour violation, $|\phi_s| < 0.05$, so that any observation of a large CP violation phase would rule out those models [20]. The analysis allows also a determination of the decay width difference predicted by the standard model to be

$$\Delta\Gamma_{s(\rm SM)} = 0.087 \pm 0.021\ \text{ps}^{-1},$$

but this quantity is expected having a reduced sensitivity to new physics processes [21].

The differential decay width is expressed as the sum of 10 functions of the time and the angles:

$$\frac{d^4\Gamma(B_s^0(t))}{d\Theta dt} = f(\Theta,\alpha,ct) \propto \sum_{i=1}^{10} O_i(\alpha,ct)\cdot g_i(\Theta)$$

$$O_i(\alpha,ct) = N_i e^{-t/\tau}\left[a_i\cosh\left(\tfrac{1}{2}\Delta\Gamma_s ct\right) + b_i\sinh\left(\tfrac{1}{2}\Delta\Gamma_s ct\right) \pm c_i\cos\left(\Delta m_s ct\right) \pm d_i\sin\left(\Delta m_s ct\right)\right]$$

i	$g_i(\theta_T,\varphi_T,\psi_T)$	N_i	a_i	b_i	c_i	d_i
1	$2\cos^2\psi_T(1-\sin^2\theta_T\cos^2\varphi_T)$	$\lvert A_0\rvert^2$	1	D	C	$-S$
2	$\sin^2\psi_T(1-\sin^2\theta_T\sin^2\varphi_T)$	$\lvert A_\parallel\rvert^2$	1	D	C	$-S$
3	$\sin^2\psi_T\sin^2\theta_T$	$\lvert A_\perp\rvert^2$	1	$-D$	C	S
4	$-\sin^2\psi_T\sin 2\theta_T\sin\varphi_T$	$\lvert A_0\rvert\lvert A_\perp\rvert$	$C\sin(\delta_\perp-\delta_\parallel)$	$S\cos(\delta_\perp-\delta_\parallel)$	$\sin(\delta_\perp-\delta_\parallel)$	$D\cos(\delta_\perp-\delta_\parallel)$
5	$\frac{1}{\sqrt{2}}\sin 2\psi_T\sin^2\theta_T\sin 2\varphi_T$	$\lvert A_0\rvert\lvert A_\parallel\rvert$	$\cos(\delta_\parallel-\delta_0)$	$D\cos(\delta_\parallel-\delta_0)$	$C\cos(\delta_\parallel-\delta_0)$	$-S\cos(\delta_\parallel-\delta_0)$
6	$\frac{1}{\sqrt{2}}\sin 2\psi_T\sin 2\theta_T\sin\varphi_T$	$\lvert A_0\rvert\lvert A_\perp\rvert$	$C\sin(\delta_\perp-\delta_0)$	$S\cos(\delta_\perp-\delta_0)$	$\sin(\delta_\perp-\delta_0)$	$D\cos(\delta_\perp-\delta_0)$
7	$\frac{2}{3}(1-\sin^2\theta_T\cos^2\varphi_T)$	$\lvert A_S\rvert^2$	1	$-D$	C	S
8	$\frac{1}{3}\sqrt{6}\sin\psi_T\sin^2\theta_T\sin 2\varphi_T$	$\lvert A_S\rvert\lvert A_\parallel\rvert$	$C\cos(\delta_\parallel-\delta_S)$	$S\sin(\delta_\parallel-\delta_S)$	$\cos(\delta_\parallel-\delta_S)$	$D\sin(\delta_\parallel-\delta_S)$
9	$\frac{1}{3}\sqrt{6}\sin\psi_T\sin 2\theta_T\cos\varphi_T$	$\lvert A_S\rvert\lvert A_\perp\rvert$	$\sin(\delta_\perp-\delta_S)$	$-D\sin(\delta_\perp-\delta_S)$	$C\sin(\delta_\perp-\delta_S)$	$S\sin(\delta_\perp-\delta_S)$
10	$\frac{4}{3}\sqrt{3}(1-\sin^2\theta_T\cos^2\varphi_T)$	$\lvert A_S\rvert\lvert A_0\rvert$	$C\cos(\delta_0-\delta_S)$	$S\sin(\delta_0-\delta_S)$	$\cos(\delta_0-\delta_S)$	$D\sin(\delta_0-\delta_S)$

$$C = \frac{1-|\lambda|^2}{1+|\lambda|^2} \qquad S = -\frac{2|\lambda|\sin\phi_s}{1+|\lambda|^2} \qquad D = -\frac{2|\lambda|\cos\phi_s}{1+|\lambda|^2}.$$

The amplitudes $A_\perp$, A_0, $A_\parallel$, $A_{\rm S}$ correspond to the P-wave and S-wave components, with their phases $\delta_\perp$, δ_0, $\delta_\parallel$, δ_S; $|\lambda|$ describes the direct CP violation. In the expression the signs of c_i and d_i coefficients are positive or negative for the decay of an initial B_s^0 or $\bar{B}_s^0$ respectively.

The differential width depends only on the differences among the phases δ, so in the fit $\delta_0 = 0$ was assumed, and the difference $\delta_{S\perp}$ between $\delta_\perp$ and δ_S was fitted as an unique variable to reduce the correlation among the parameters. No direct violation was assumed in the measurement, therefore $|\lambda| = 1$ was fixed.

The discrimination between the positive or negative initial flavour is obtained looking for a second B produced in the event and inferring its flavour looking at the charge of its decay products; of course the charge-flavour correlation is diluted due to the presence of cascade decays and oscillations of the other b hadron itself.

In ATLAS analysis [22] of $\sqrt{s} = 7$ TeV data the flavour was tagged looking at the charge of particles contained in a cone around a muon, assumed to come from the semileptonic decay of a b; if no muon was found the particles in a b-tagged jets were used. A "cone charge" was defined as

$$Q = \frac{\sum_i^{N_{\text{tracks}}} q^i \cdot (p_{T,i})^j}{\sum_i^{N_{\text{tracks}}} (p_{T,i})^j}$$

where $j = 1.1$ and the sum was performed over the reconstructed tracks within a cone size of $\Delta R = 0.5$.

In CMS analysis [23] of $\sqrt{s} = 8$ TeV data only semileptonic decays were used to tag the flavour, looking to both electrons and muons. The performance of the methods were measured with events containing the self-tagging decay $B^+ \to J/\psi K^+$. The efficiency and tagging power of the algorithms are reported in tab.3

Table 3: Performance of flavour tagging algorithm in CMS analysis; errors are statistical only.

	ATLAS	CMS
Tagging efficiency $\epsilon_{\text{tag}}(\%)$	32.1 ± 0.01	7.67 ± 0.04
Mistag fraction $\omega(\%)$	21.3 ± 0.08	32.2 ± 0.3
Tagging power $P_{\text{tag}}(\%)$	1.45 ± 0.05	0.97 ± 0.03

The results of an unbinned maximum likelihood fit, including per-event resolution and tagging probability terms are shown in tab.4 and fig.9.

Table 4: Final results of CP violating phase and decay width difference measurements.

	ATLAS	CMS
ϕ_s[rad]	$0.12 \pm 0.25 \pm 0.05$	$-0.03 \pm 0.11 \pm 0.03$
$\Delta\Gamma_s$[ps^{-1}]	$0.053 \pm 0.021 \pm 0.010$	$0.096 \pm 0.014 \pm 0.007$

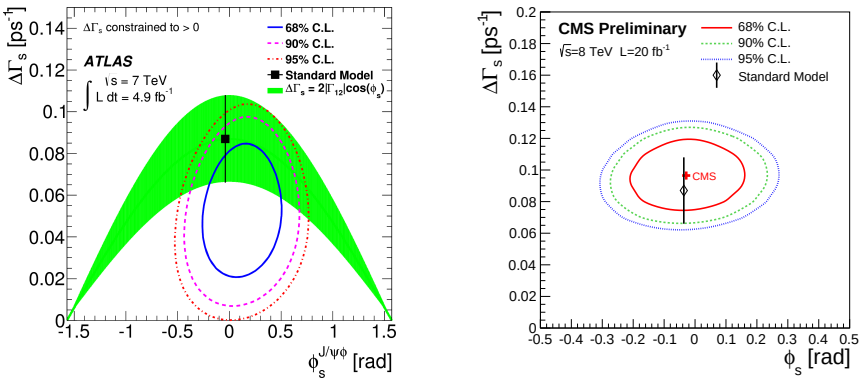

Figure 9 – Likelihood contours in the $\phi_s - \Delta\Gamma_s$ plane in ATLAS (left) and CMS (right) measurements.

Both experiments found a result in agreement with the prediction, but a significant test will require a smaller uncertainty, so further investigations are required.

Again, more data will be available with the new run and increased luminosity, but this will correspond to a more difficult environment. ATLAS will have an improved pixel tracker, with a fourth layer, for Run2, and a new tracker with reduced pixel size for HL-LHC. The need to stay inside a necessarily limited trigger bandwidth will require harder cuts on muon p_T; two possible cuts have been considered, at 6 GeV for Phase-1 and 11 GeV for Phase-2. The upgraded tracker will allow a better vertex reconstruction and an improvement of 30% in proper decay time resolution. In principle this could be affected by the higher pileup, but a dedicated study [24] showed that even in the hypothesis that the number of interaction could reach $N = 200$, no significant effect appears visible, as shown in fig.10.

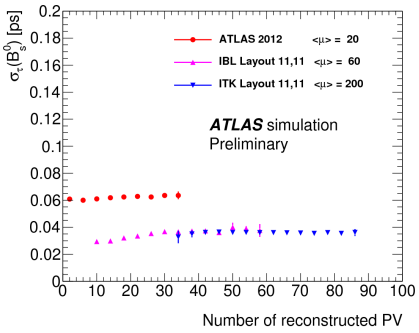

Figure 10 – Proper decay time resolution in ATLAS against the number of reconstructed primary vertices in simulated $B_s^0 \to J/\psi\phi$ events.

Estimating the signal yields applying the harder muon p_T cuts to 2012 data and rescaling with efficiencies and luminosities the results shown in tab.5 are obtained.

Table 5: Estimated ATLAS statistical precisions of ϕ_s measurement for considered LHC periods.

$\mathcal{L}(\text{fb}^{-1})$	$p_{T\mu}$ cut [GeV]	$\sigma(\phi_s)$(stat)[rad]
100	6	0.054
100	11	0.10
250	11	0.064
3000	11	0.022

3.2 $B_s^0 \to J/\psi f_0$ decay

Another channel that can be studied to investigate CP violation is $B_s^0 \to J/\psi f_0$; the f_0 is a scalar and the final state is an almost pure CP-odd eigenstate, so that there's no need to disentangle two components and no angular analysis is required:

$$\Gamma(B_s^0/\bar{B}_s^0 \to J/\psi f_0) = \mathcal{N} e^{-\Gamma_s t}\left\{e^{\Delta\Gamma_s t/2}(1+\cos\phi_s) + e^{-\Delta\Gamma_s t/2}(1-\cos\phi_s) \pm \sin\phi_s \sin(\Delta m_s t)\right\}$$

On the other side the hadronic corrections to apply in predictions depend on the structure of the f_0, that is not completely clear, as it could be a simple quark-antiquark pair, but also a tetraquark or a KK molecule [25]. In the analysis, the initial flavour can be tagged using the same techinque used as for $B_s^0 \to J/\psi\phi$, and the tagging information is to be added to the $\sin\phi_s$ term.

This analysis has not yet been performed, but some propaedeutic study has been done. The branching fraction ratio $\mathcal{B}(B_s^0 \to J/\psi f_0)\mathcal{B}(f_0 \to \pi^+\pi^-)/\mathcal{B}(B_s^0 \to J/\psi\phi)\mathcal{B}(\phi \to K^+K^-)$ has been measured by CMS [26], while the lifetime and CP violation measurements are to come.

This is not only a necessary experimental exercise but is useful to give informations about the hadronic structure of the f_0. Events were selected requiring a dimuon originating from a displaced secondary vertex, to form a J/ψ, and two opposite charged pions to form a f_0 candidate or two kaons to form a ϕ. The $J/\psi\pi^+\pi^-$ invariant mass distribution is shown in fig.11.

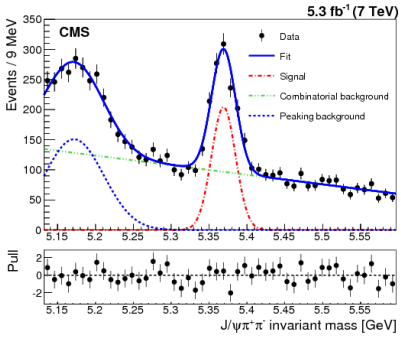

Figure 11 – Invariant mass distribution of the $B_s^0 \to J/\psi f_0$ candidates.

As a ratio is measured, again there's a cancellation of systematic uncertainties; yields were measured using an unbinned maximum likelihood fit and efficiencies were computed from simulation. The final result is

$$R_{f_0/\phi} = \frac{\mathcal{B}(B_s^0 \to J/\psi f_0)\mathcal{B}(f_0 \to \pi^+\pi^-)}{\mathcal{B}(B_s^0 \to J/\psi\phi)\mathcal{B}(\phi \to K^+K^-)} = 0.140 \pm 0.013 \pm 0.018$$

4 Conclusions

ATLAS and CMS have produced significant EW results in HF physics: $\mathcal{B}(B_s^0 \to \mu^+\mu^-)$ have been measured, an angular analysis of $B^0 \to K^{*0}\mu^+\mu^-$ have been performed, the CP violation phase ϕ_s in $B_s^0 \to J/\psi\phi$ decay has been measured and the study of the $B_s^0 \to J/\psi f_0$ decay begun.

All results are, up to now, compatible with SM predictions, but more stringent tests will be obtained with more precise measurement to be done in the future LHC runs.

References

1. C.Bobeth *et al.*, $B_{s,d} \to \ell^+\ell$ in the Standard Model with Reduced Theoretical Uncertainty, *Phys. Lett.* B **112**, 101801 (2014). doi: 10.1103/PhysRevLett.112.101801
2. J.R.Ellis *et al.*, On $B_s^0 \to \mu^+\mu^-$ and cold dark matter scattering in the MSSM with non-universal Higgs, *J. High Energy Phys.* **05**, 063 (2006). doi: 10.1088/1126-6708/2006/05/063
3. S.Davidson and S. Descotes-Genon, "Minimal Flavour Violation" for leptoquarks, *J. High Energy Phys.* **11**, 073 (2010). doi: 10.1007/JHEP11(2010)073
4. S. R. Choudhury *et al.*, SIGNATURES OF NEW PHYSICS IN DILEPTONIC B-DECAYS, *Int. J. Mod. Phys.* A **21**, 2017 (2006). doi: 10.1142/S0217751X06029491
5. J.K.Parry, Lepton flavour violating Higgs boson decays, $\tau \to \mu\gamma$ and $B_s^0 \to \mu^+\mu^-$ in the constrained MSSM + ν_R with large $\tan\beta$, *Nucl. Phys.* B **760**, 38 (2006). doi: 10.1016/j.nuclphysb.2006.10.011
6. J.R.Ellis *et al.*, B-meson observables in the maximally CP-violating MSSM with minimal flavor violation, *Phys. Rev.* D **76**, 115011 (2007). doi: 10.1103/PhysRevD.76.115011
7. G.D'Ambrosio *et al.*, Minimal flavour violation: an effective field theory approach, *Nucl. Phys.* B **645**, 155 (2002). doi: http://dx.doi.org/10.1016/S0550-3213(02)00836-2

8. LHCb Collaboration, Measurement of the fragmentation fraction ratio f_s/f_d and its dependence on B meson kinematics, *J. High Energy Phys.* **04**, 001 (2013) doi: http://dx.doi.org/10.1007/JHEP04(2013)001
9. LHCb Collaboration, Average f_s/f_d b-hadron production fraction ratio for $\sqrt{s} = 7$ TeV collisions, Jul, 2013
10. ATLAS Collaboration, Limit on $B_s^0 \to \mu^+\mu^-$ branching fraction based on 4.9 fb^{-1} of integrated luminosity, ATLAS-CONF-2013-076. url: http://atlas.web.cern.ch/Atlas/GROUPS/PHYSICS/CONFNOTES/ATLAS-CONF-2013-076
11. CMS and LHCb Collaborations, Observation of the rare $B_s^0 \to \mu^+\mu^-$ decay from the combined analysis of CMS and LHCb data, arXiv:1411.4413. url: http://arxiv.org/pdf/1411.4413v1.pdf
12. CMS Collaboration, Measurement of the $B_s^0 \to \mu^+\mu^-$ Branching Fraction and Search for $B^0 \to \mu^+\mu^-$ with the CMS Experiment, *Phys. Rev. Lett.* **111**, 101804 (2013). doi: 10.1103/PhysRevLett.111.101804
13. A.Khodjamirian *et al.*, Form factors and strong couplings of heavy baryons from QCD light-cone sum rules, *J. High Energy Phys.* **09**, 106 (2011). doi: http://dx.doi.org/10.1007/JHEP09(2011)106
14. CMS Collaboration, Physics Performance for 2$^{\text{nd}}$ ECFA workshop. url: https://twiki.cern.ch/twiki/pub/CMSPublic/PhysicsResultsFP/ECFA-CMSPublicResults.pdf
15. W.Altmannshofer *et al.*, Symmetries and asymmetries of $B^0 \to K^{*0}\mu^+\mu^-$ decays in the Standard Model and beyond, *J. High Energy Phys.* **01**, 019 (2009). doi: 10.1088/1126-6708/2009/01/019
16. ATLAS Collaboration, Angular analysis of $B^0 \to K^{*0}\mu^+\mu^-$ with the ATLAS Experiment, ATLAS-CONF-2013-038. url: https://atlas.web.cern.ch/Atlas/GROUPS/PHYSICS/CONFNOTES/ATLAS-CONF-2013-038
17. BaBar collaboration, Time-integrated and time-dependent angular analyses of $B \to J/\psi K\pi$: A measurement of $\cos 2\beta$ with no sign ambiguity from strong phases, *Phys. Rev.* D **71**, 032005 (2005). doi: http://dx.doi.org/10.1103/PhysRevD.71.032005
18. CMS Collaboration, Angular analysis and branching fraction measurement of the decay $B^0 \to K^{*0}\mu^+\mu^-$, *Phys. Lett.* B **727**, 77 (2013). doi: 10.1016/j.physletb.2013.10.017
19. J.Charles *et al.*, Predictions of selected flavor observables within the standard model, *Phys. Rev.* D **84**, 033005 (2011). doi: 10.1103/PhysRevD.84.033005
20. G.Isidori, Flavor physics and CP violation, arXiv:1302.0661. url: http://arxiv.org/pdf/1302.0661v1.pdf
21. A.Lenz and U.Nierste, Numerical updates of lifetimes and mixing parameters of B mesons, arXiv:1102.4274. url: http://arxiv.org/pdf/1102.4274v1.pdf
22. ATLAS Collaboration, Flavor tagged time-dependent angular analysis of the $B_s^0 \to J/\psi\phi$ decay and extraction of $\Delta\Gamma_s$ and the weak phase ϕ_s in ATLAS, *Phys. Rev.* D **90**, 052007 (2014). doi: 10.1103/PhysRevD.90.052007
23. CMS Collaboration, Measurement of the CP-violating weak phase ϕ_s and the decay width difference $\Delta\Gamma_s$ using the $B_s^0 \to J/\psi\phi(1020)$ decay channel, CMS-PAS-BPH-13-012. url: http://cds.cern.ch/record/1744869/files/BPH-13-012-pas.pdf
24. ATLAS Collaboration, ATLAS B-physics studies at increased LHC luminosity, potential for CP-violation measurement in the $B_s^0 \to J/\psi\phi$ decay, ATL-PHYS-PUB-2013-010. url: http://cds.cern.ch/record/1604429/files/ATL-PHYS-PUB-2013-010.pdf
25. R.Fleischer *et al.*, Anatomy of $B_s^0 \to J/\psi f_0(980)$, *Eur. Phys. J.* C **71**, 1832 (2011). doi: 10.1140/epjc/s10052-011-1832-x
26. CMS Collaboration, Measurement of the ratio $\mathcal{B}(B_s^0 \to J/\psi f_0)/\mathcal{B}(B_s^0 \to J/\psi\phi(1020))$ in pp collisions at $\sqrt{s} = 7$ TeV, arXiv:1501.06089. url: http://arxiv.org/pdf/1501.06089v1.pdf